Available online at www.sciencedirect.com
ScienceDirect
Earth and Planetary Science Letters 260 (2007) 242–256
EPSL
www.elsevier.com/locate/epsl

Reducing role of sulfides and diamond formation in the Earth's mantle

Yu.N. Palyanov *, Yu.M. Borzdov, Yu.V. Bataleva, A.G. Sokol, G.A. Palyanova, I.N. Kupriyanov

Institute of Geology and Mineralogy, Siberian Branch of the Russian Academy of Sciences, Academician Koptyug ave., 3, 630090 Novosibirsk, Russia

Received 20 January 2007; received in revised form 10 May 2007; accepted 19 May 2007
Available online 26 May 2007
Editor: G.D. Price

Abstract

Sulfides are abundant inclusions in diamond, but their role in the diamond genesis is still debatable. To address this issue, experimental modeling of natural diamond-forming processes with the participation of sulfides has been performed with the $MgCO_3$–SiO_2–Al_2O_3–FeS system at 6.3 GPa in the temperature range of 1250–1800 °C, using a multi-anvil high pressure apparatus of the "split-sphere" type. As a result of redox reactions involving carbonate, oxides and sulfide, diamond and/or graphite are produced in association with garnet, orthopyroxene, coesite and sulfides (pyrite, pyrrhotite). Diamond crystals, formed from the carbon of initial carbonate, are found to contain nitrogen impurity with total concentration of approximately 1500 ppm, and defects related to hydrogen impurity. Based on the experimental data and thermodynamic calculations, the processes of the carbonate–oxide–sulfide interaction are reconstructed, revealing the role of sulfides as a reducing agent for CO_2-fluid. It is established that pyrrhotite acts as the reducing agent irrespective of its aggregate state (solid or melt). At temperatures below melting, pyrrhotite is enriched with sulfur and depleted with iron from FeS to $Fe_{0.85}S$. At higher temperatures, sulfide melt is enriched with sulfur and crystallizes as pyrite and pyrrhotite during quenching. The medium in which diamond and/or graphite crystallize is a CO_2-dominated fluid containing dissolved carbon, silicates, oxides and sulfides. The investigated processes and mechanisms of diamond crystallization can be considered as a possible model of the diamond formation in sulfide-bearing paragenesis in mantle metasomatism or UHP metamorphism of crustal material.

Keywords: diamond formation; sulfides; carbonates; silicates; fluid; redox reactions; mantle; HPHT experiments

1. Introduction

The modern models of diamond genesis are based, mainly, on the results of investigations of mineral and fluid inclusions in diamonds, as well as on experimental data on diamond formation in various media. Among the mineral inclusions in diamond, silicates, sulfides and oxides dominate (Sobolev, 1977; Meyer, 1987; Harris, 1992). Fluid inclusions in diamonds have been actively studied since recent time, because it is fluid inclusions that give an exceptionally significant information for the reconstruction of diamond-forming media (Navon et al., 1988; Schrauder and Navon, 1993, 1994; Izraeli et al.,

* Corresponding author. Tel./fax: +7 383 330 75 01.
E-mail address: palyanov@uiggm.nsc.ru (Y.N. Palyanov).

0012-821X/$ - see front matter © 2007 Elsevier B.V. All rights reserved.
doi:10.1016/j.epsl.2007.05.033

2001). Of particular interest are micro- and nano-inclusions, characteristic of diamonds of both mantle (Klein-BenDavid et al., 2006; Tomlinson et al., 2006) and UHP metamorphic origin (Dobrzhinetskaya et al., 2003; Hwang et al., 2005). A comprehensive body of data accrued from the inclusion studies demonstrates the complexity and heterogeneity of the natural diamond-forming environment. This stimulates experimental investigations aimed at determining the role of specific components of the environment in nucleation and growth of diamond. Since, most of the models associate the origin of diamond with oxidation–reduction reactions (Haggerty, 1986; Sobolev and Shatsky, 1990; Deines and Harris, 1995; Ogasawara et al., 1997; Luth, 1999) and mantle metasomatism (Boyd et al., 1994a,b; Taylor and Anand, 2004; Shatsky et al., 2005), experimental studies into these reactions and processes are of interest.

At the opening stage of the experimental modeling of the diamond genesis, various non-metallic solvents have been investigated for the capability of diamond synthesis. These include melts of alkaline (Akaishi et al., 1990; Litvin et al., 1997; Pal'yanov et al., 1999) and alkaline–earth carbonates (Akaishi et al., 1990; Taniguchi et al., 1996; Pal'yanov et al., 1998; Sato et al., 1999), carbonate–silicate systems (Arima et al., 1993; Litvin and Zharikov, 2000; Shatsky et al., 2002), sulfide melts (Litvin et al., 2002; Palyanov et al., 2006) and sulfur (Sato and Katsura, 2001; Pal'yanov et al., 2001). Since fluids are believed to play an important role in diamond formation processes, diamond crystallization has been studied in C–O–H system (Yamaoka et al., 1992; Akaishi et al., 2000; Sokol et al., 2001), silicate–fluid (Sokol et al., 1999; Pal'yanov et al., 2005a) and carbonate–fluid systems (Pal'yanov et al., 1999, 2002a; Sokol et al., 2004). Recently, experimental studies focusing on diamond formation through oxidation–reduction reactions have started to appear. To date it has been experimentally demonstrated that diamond can form as a result of redox reactions involving carbonates and Si, SiC or silicon-bearing metal (Arima et al., 2002; Siebert et al., 2005), or carbonates and reduced fluids (Pal'yanov et al., 2002b; Yamaoka et al., 2002; Pal'yanov et al., 2005b).

One of the challenging questions is unrevealed role of sulfides in the origin of diamond. As is known, sulfides are among the most common inclusions in diamonds (Sharp, 1966; Harris and Gurney, 1979; Efimova et al., 1983; Bulanova et al., 1993; Pearson et al., 1998; Richardson et al., 2004). A considerable amount of sulfide micro-inclusions were revealed in diamonds from kimberlites from Canada and Siberia (Klein-BenDavid et al., 2003, 2006) as well as in metamorphic diamonds from Erzgebirge (Hwang et al., 2001) and Kokchetav Massif (Hwang et al., 2003). Two models have been proposed, which account for the involvement of sulfides in diamond genesis. First one supposes diamond crystallization from sulfide melt saturated with carbon (Haggerty, 1986), in a manner similar to diamond synthesis from carbon solution in transition metals melt. This model has been developed in a number of studies (Bulanova et al., 1993; Bulanova, 1995; Spetsius, 1999). Experiments on the interaction between graphite and sulfide melts of FeS and $(Fe,Ni)_9S_8$ compositions, performed over a wide range of P–T parameters, showed that the minimal pressure required for diamond nucleation from carbon saturated sulfide melt is 7.5 GPa (Palyanov et al., 2006). Another idea was first proposed by Marx (Marx, 1972), who suggested that diamond could form via the reaction $2FeS+CO_2=2FeO+S_2+C$. Experimental investigation of this or similar reactions, however, represents a formidable task due to methodical complexity. First study along this line is the experimental investigation of magnesite reduction in the presence of a eutectic-composition $Fe_{70}S_{28}O_2$ melt (Gunn and Luth, 2006). As a result of carbonate reduction by Fe^0-rich sulfide melt metastable graphite was produced in the experiments.

In the present study, we have investigated carbonate–oxide–sulfide interaction in the $MgCO_3$–SiO_2–Al_2O_3–FeS system under mantle P–T parameters. Based on the experimental data and thermodynamic calculations an

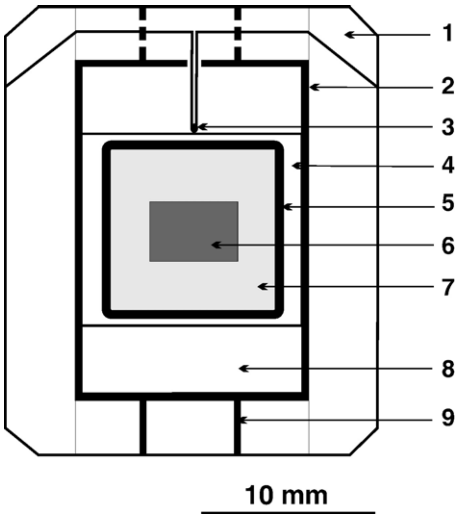

Fig. 1. The high pressure cell used in the present study: 1 — ZrO_2 container; 2 — cylindrical graphite heater; 3 — $PtRh_6/PtRh_{30}$ thermocouple; 4 — MgO sleeve; 5 — graphite sleeve; 6 — FeS; 7 — $MgCO_3+Al_2O_3+SiO_2$ ampoule; 8 — ZrO_2; 9 — Mo leads.

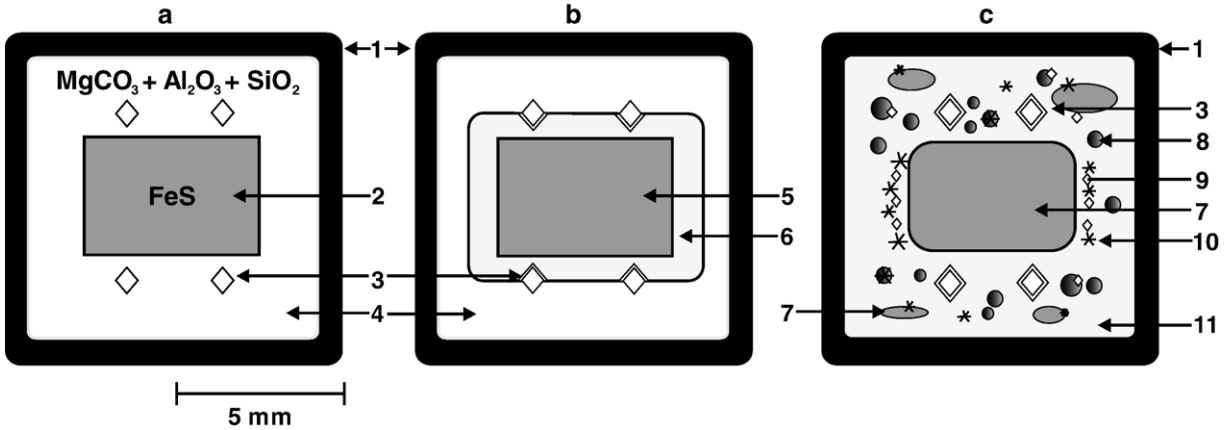

Fig. 2. Schemes of carbonate–oxide–sulfide interaction in the reaction ampoules. a — initial ampoule assembly; b — scheme of ampoule at 1250–1450 °C; c — scheme of ampoule at 1600–1800 °C. 1 — graphite sleeve; 2 — pyrrhotite; 3 — diamond seed crystal; 4 — carbonate–oxide ampoule; 5 — pyrrhotite; 6 — reaction zone; 7 — quenched pyrite–pyrrhotite aggregate; 8 — cavity; 9 — spontaneous diamond crystals; 10 — metastable graphite; 11 — polycrystalline garnet aggregate.

attempt to unravel the role of sulfides and determine possible mechanisms of diamond formation has been made.

2. Experimental methods

Experiments were carried out using a multi-anvil high-pressure apparatus of a "split-sphere" type (Pal'yanov et al., 1997). A high-pressure cell (Fig. 1) in the form of tetragonal prism, 21.1×21.1×25.4 mm in size, was used. The temperature was measured in each experiment using a $PtRh_{30}/PtRh_6$ thermocouple. Details on the pressure and temperature calibration have been presented elsewhere (Pal'yanov et al., 2002a).

The methodical approach and corresponding scheme of the reaction ampoule assembly were developed to realize in the course of experiments the decarbonation reaction, releasing CO_2, and then (or in parallel) to create conditions for the interaction between CO_2 and sulfide. As a result, the scheme, shown in Fig. 2a, was adopted. Ampoules, with a height of 9.2 mm, outer diameter of 9.5 mm and wall thickness of 2.2 mm, were made from a

Table 1
Experimental results

Run	T (°C)	Time (h)	Sleeve material	Final phases (X-ray)		Carbon phases	Diamond growth on seeds
				Silicates, carbonates	Sulfides		
85/8	1700	23.5	MgO+Pt	Grt+OPx+Ol+Ky	[a]	G+D	Yes
126/8	1500	44	MgO+BN	Grt+[b]	Po_{qu}	G	Yes
125/8	1600	42	MgO+BN	Grt+Ol+Cor+[b]	Po_{qu}	G	Yes
97/8	1700	15	MgO+BN	Grt+Ol+OPx+[b]	Po_{qu}	G+D	Yes
134/8	1250	42	MgO+G	Ms+Grt+Co+Ky	Po	G	Yes
130/8	1350	42.5	MgO+G	Ms+Grt+Co+Ky	Po	G	Yes
129/8	1450	42	MgO+G	Ms+Grt+Co+Ky	Po	G	Yes
88/8	1600	23.5	MgO+G	Grt+Co+Ms+Ky+OPx	$Po_{qu}+Py_{qu}$	G	Yes
92/8	1650	23.5	MgO+G	Grt+Co+OPx	$Po_{qu}+Py_{qu}$	G+D	Yes
90/8	1700	8	MgO+G	Grt+Co+OPx+Ky	$Po_{qu}+Py_{qu}$	G+D	Yes
91/8	1800	8	MgO+G	Grt	$Po_{qu}+Py_{qu}$	G	No

Notes: Grt — garnet, Ms — magnesite, Co — coesite, Cor — corundum, OPx — orthopyroxene, Ky — kyanite, Ol — olivine, Py — pyrite, Po — pyrrhotite, G — graphite, D — spontaneously nucleated diamond; Po_{qu} , Py_{qu} — quenching phases.

[a] PtS+(Fe,Pt)S — products of interaction of FeS with the sleeve material.

[b] $Mg_3B_2O_6+Mg_2B_2O_5$ — oxidation products in sleeves after experiments.

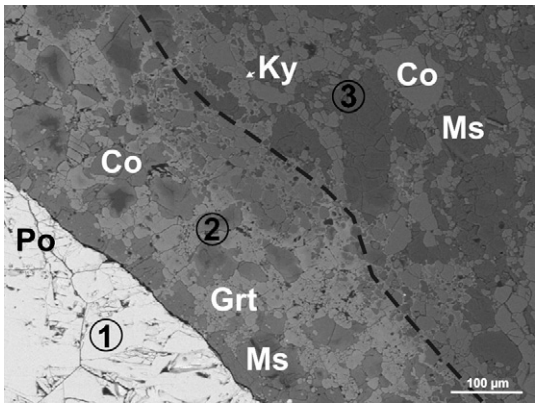

Fig. 3. SEM micrograph of the polished section (run 134/8, 1250 °C) with microprobe analysis data. 1 — sulfide; 2 — reaction zone, containing garnet, magnesite and coesite; 3 — outer part of the ampoule, consisting of magnesite, coesite and kyanite. Notes: Grt — garnet, Ky — kyanite, Ms — magnesite, Co — coesite, Po — pyrrhotite.

mixture of $MgCO_3$ (359 mg), Al_2O_3 (143 mg), and SiO_2 (335 mg). In molar proportions the starting mixture had Mg:Al:Si of 3:2:4. Reacting completely under the run conditions, this mixture would produce pyrope and small amount of enstatite and coesite, due to small excess of silica. A FeS pellet with diameter of 5 mm, height of 3.5 mm and mass of 300 mg, was placed inside the ampoule. Cubo-octahedral synthetic diamond seed crystals approximately 0.5 mm in size were placed in the carbonate–oxide ampoule, as shown in Fig. 2a. The starting materials were natural magnesite (Chelyabinsk Region, Russia) with an impurity content of 0.5 wt.% and 99.9% pure SiO_2 and Al_2O_3. Stoichiometric pyrrhotite was synthesized by heating a mixture of iron (99.99%) and sulfur (99.99%) in evacuated quartz ampoules at 750 °C for 48 h.

Taking into account high reactivity of sulfides the reaction charge was isolated from the graphite heater using double sleeves. Three compositions of the sleeves, including MgO+Pt, MgO+BN, MgO+graphite were employed. BN-capsules were made by pressing pure h-BN powder without any binder. As it will be shown below the optimal composition was MgO+graphite. At the same time, since the results obtained with the other sleeves may represent an independent interest, some typical examples illustrating the effect of the isolation materials are also presented in the paper.

After experiments, samples were studied using optical microscopy and scanning electron microscopes LEO420 and LEO1430VP. Phase composition of the samples from different parts of the reaction ampoules was determined by X-ray (a DRON-3 diffractometer) and microprobe (Camebax-Micro) analyses. For microprobe analysis samples in the form of polished sections were prepared. Infrared absorption spectra of diamonds were measured using a Bruker Vertex 70 FTIR spectrometer fitted with a Hyperion 2000 IR microscope. The isotopic analysis of carbon was performed using an isotope ratio mass-spectrometer Finnigan MAT 253 equipped with an EA1112 elemental analyzer.

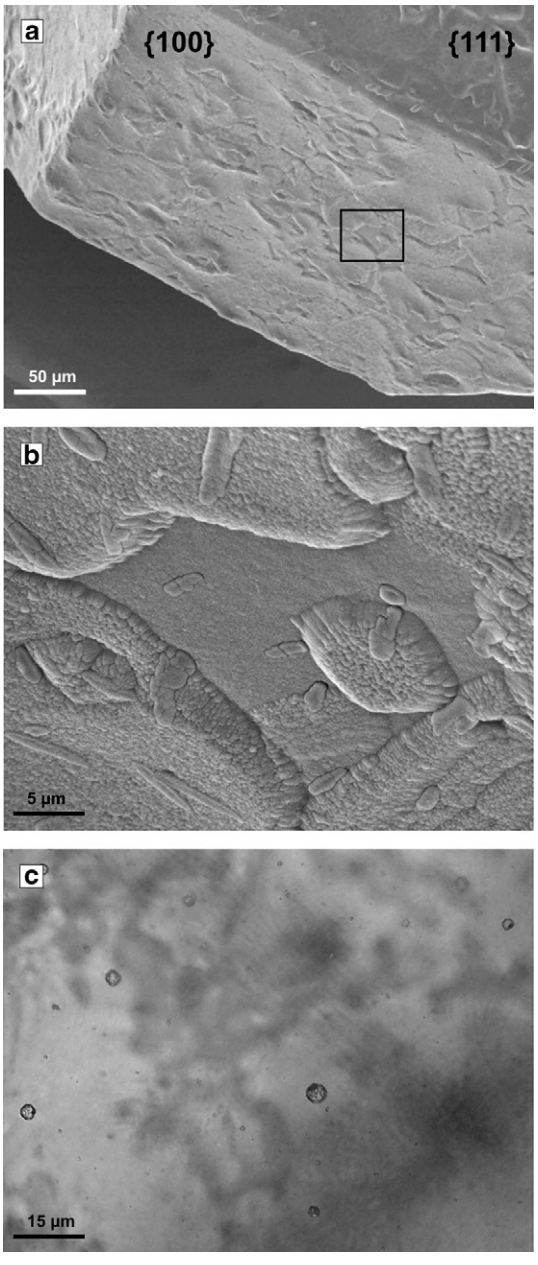

Fig. 4. SEM micrographs: a — cubo-octahedral diamond seed crystal with overgrown layers (run 134/8, 1250 °C); b — an expanded fragment of the Fig. a, showing {100} face with growth features. c — Optical micrograph, showing transparent inclusions in the overgrown layer located at the depth of 5 μm.

3. Results

3.1. Experiments on the carbonate–oxide–sulfide interaction

The results of experiments on the carbonate–oxide–sulfide interaction are presented in Table 1. Isolation of the reaction charge with a (MgO+Pt) sleeve (run 85/8) yielded FePt, PtS, and (Fe,Pt)S phases in the run products, indicating that pyrrhotite reacted with Pt. Application of a double sleeve composed of MgO and BN (run 126/8) also resulted in formation of additional phases, namely $Mg_3B_2O_6$ and $Mg_2B_2O_5$. Therefore, in order to exclude penetration of extra chemical agents to the reaction volume, a double isolation sleeve composed of MgO and machined graphite (MgO+G) was applied in the main series of experiments.

Experiments, using composite (MgO+G) isolation sleeves, were carried out at a pressure of 6.3 GPa and temperatures in the range of 1250–1800 °C with a duration from 8 to 42.5 h. At 1250 °C (run 134/8) it was established that in the inner part of the carbonate–oxide ampoule at the contact with sulfide, the initial phases reacted to form garnet, kyanite and graphite. In the outer part of the ampoule only magnesite, coesite and kyanite were found, indicating that no decarbonation reaction took place. An analysis of the spatial distribution of the coexisting phases showed that within the reaction zone the occurrence of garnet and kyanite had a mutually exclusive character; areas rich in garnet did not show kyanite and vice versa (Fig. 3). This occurrence pattern is in agreement with the phase assemblage expected from the stoichiometry of the starting mixture. Diamond growth was established on the {100} and {111} faces of the seed crystals located within the reaction zone (Figs. 2b and 4). As the temperature increased from 1250 to 1450 °C the width of the reaction zone was found to increase. In the run products the quantity of unreacted carbonate and oxides decreased and quantity of metastable graphite increased. In this temperature range sulfide did not melt and was identified after experiments as pyrrhotite.

At 1600 °C (run 88/8) melting of sulfide was established. An X-ray analysis showed that pyrite and

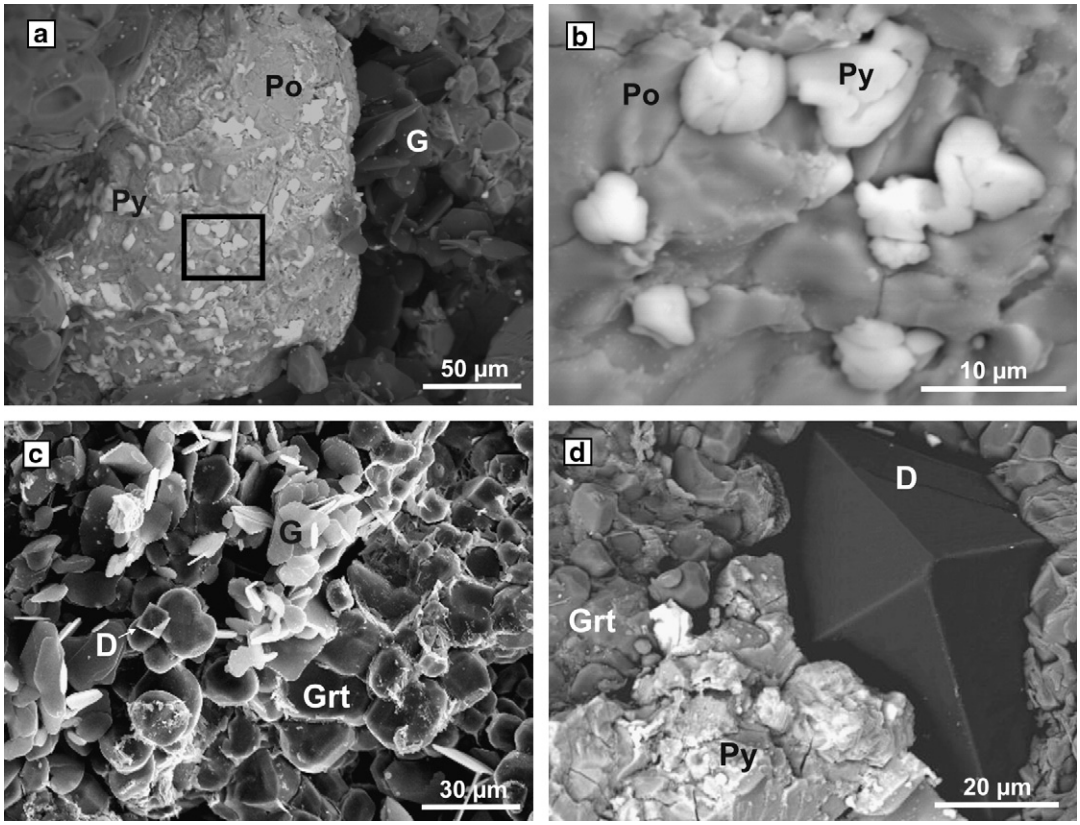

Fig. 5. SEM micrographs: a — pyrite–pyrrhotite quenched aggregate (run 88/8, 1600 °C); b — an expanded fragment of the Fig. a; c — fragment of carbonate–silicate ampoule (run 92/8, 1650 °C); d — diamond crystal in the garnet–pyrite aggregate (run 90/8, 1700 °C). Grt — garnet, Py — pyrite, Po — pyrrhotite, G — graphite, D — spontaneously nucleated diamond.

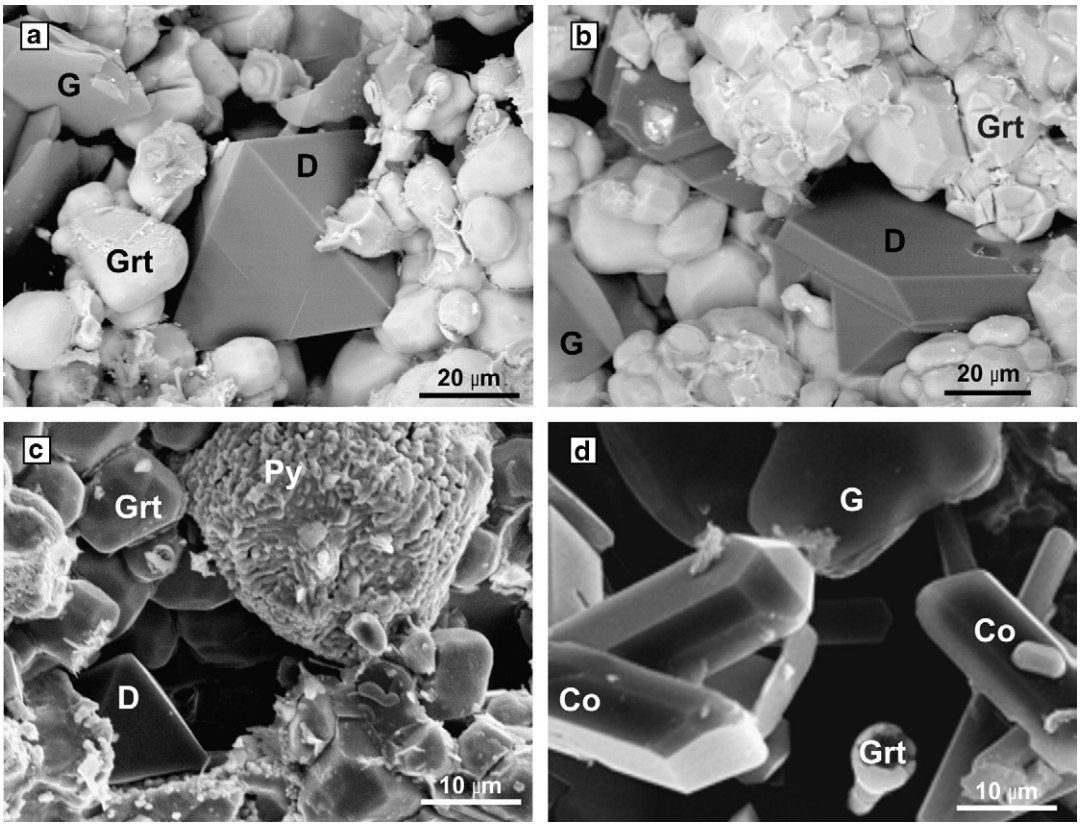

Fig. 6. SEM micrographs: a, b — diamond crystals in the polycrystalline garnet aggregate (run 90/8, 1700 °C); c — diamond crystal, garnet and pyrite in a cavity (run 92/8, 1650 °C); d — coesite, garnet and graphite crystals in a cavity (run 92/8, 1650 °C). Grt — garnet, Co — coesite, Py — pyrite, G — graphite, D— spontaneously nucleated diamond.

pyrrhotite were present in the central part of the ampoule. Sulfide was found to penetrate into carbonate–silicate substrate (Fig. 5a, b). In the run products a considerable quantity of metastable graphite and diamond growth on the seed crystals were established.

Spontaneous diamond crystallization was established at 1650 and 1700 °C (runs 92/8 and 90/8, respectively). In these experiments the initial carbonate was exhausted completely in the reactions, and a grey polycrystalline aggregate, composed of garnet, orthopyroxene, coesite, pyrite, pyrrhotite, graphite and diamond (Fig. 5c, d) was produced. The aggregate contained numerous microcavities. Inside these cavities euhedral crystals of garnet, diamond and, sometimes, coesite were found (Fig. 6a–d). At the same time, some cavities were empty. This may be explained assuming that the cavities were formed nonsimultaneously in the course of experiments.

In the products of run 91/8, performed at 1800 °C in the graphite stable region, garnet, pyrite, pyrrhotite and graphite were found. This is evidence for the completion of the decarbonation reaction and crystallization of elemental carbon exclusively in the form of graphite. These data also confirm the accuracy of the pressure and temperature measurements providing reference to the diamond–graphite equilibrium line (Fig. 7). For this experiment maximal number of cavities, with sizes from 0.1 to 1 mm was established in the silicate matrix (Fig. 8a–d). Inside the cavities, aggregates of graphite crystals, sometimes as intergrowths with garnet (Fig. 8a, b) were found. In addition, pyrite spheres, formed apparently during quenching, were frequently observed (Fig. 8b).

Summarizing experimental data on diamond formation, it is necessary to note that at relatively low temperatures, 1250–1450 °C, only diamond growth on the seed crystals was established. Furthermore, diamond growth was observed only with those seed crystals, which were located within zones, where the decarbonation reaction and formation of garnet and other phases took place (Fig. 2b). Those seed crystals (or part of them), located in carbonate–oxide zone, where the initial reagents did not react, underwent partial dissolution. At higher temperatures (Table 1) spontaneously

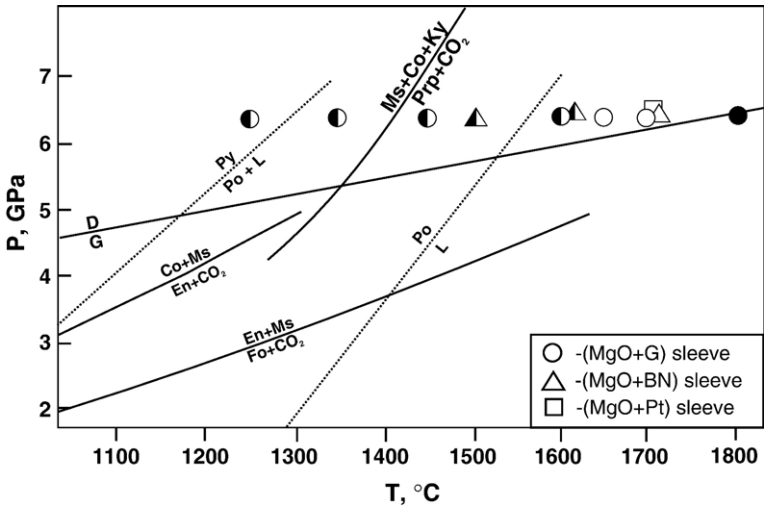

Fig. 7. Experimental results of the carbonate–oxide–sulfide interaction. Filling of symbols denotes variations in phases of carbon: solid — graphite, half black — graphite+diamond growth on seed crystals, open — spontaneously nucleated diamond+graphite+diamond growth on seed crystals. Experimentally determined decarbonation reactions are taken from Knoche et al. (1999) and Newton and Sharp (1975), decomposition curve for pyrite and melting curve for pyrrhotite are taken from Sharp (1969). Prp — pyrope, Ms — magnesite, Co — coesite, En — enstatite, Ky — kyanite, Fo — forsterite, Py — pyrite, Po — pyrrhotite, G — graphite, D — diamond.

nucleated diamond crystals were established. Diamonds were found in the silicate ampoule, but were never observed inside the sulfide pellet (Fig. 2c). Octahedral diamond crystals with sizes up to 150 μm, flattened crystals up to 80 μm or diamond intergrowth aggregates up to 400 μm were located in polycrystalline garnet aggregate (Fig. 5c), garnet–pyrite aggregate (Fig. 5d) or in the cavities (Fig. 6a–c).

3.2. Composition of silicates and sulfides

At temperatures of 1250–1450 °C, the decarbonation process was localized within the reaction zones at the contact with sulfide (Fig. 2b). Garnets formed within these zones were found to be enriched with FeO up to 29.9 wt.% (Table 2). Particular variations of Fe content were observed for garnets crystallized at 1250 °C (Fig. 9a). Microprobe analysis of garnets located in different parts of the reaction zone showed that their Fe content correlated with the distance from the pyrrhotite pellet. In general, garnets located closer to the pyrrhotite showed higher Fe concentrations. At higher temperatures (1600–1800 °C) garnet crystallized throughout the carbonate–oxide ampoule. In this case, FeO content decreased to 9–13 wt.% (Table 2). It is of interest that in experiments with the (MgO+BN) isolation sleeves, performed at similar temperatures, Fe content in garnet varied within 1–4 wt.%.

Si content in garnets and, consequently, content of pyroxene components in solid solution, increased considerably with temperature (Fig. 9b, Table 2). In garnets coexisting with orthopyroxene, crystallized at 1700–1800 °C, Si content per formula unit was up to 3.07–3.09. This implies that the composition of these garnets crystallized at 6.3 GPa, in Si content, lies within the field of majoritic garnet, which is characteristic for essentially higher pressures (Gasparik, 2002). It should be noted that garnets produced in experiments with the (MgO+G) and (MgO+BN) isolation sleeves at similar temperatures had comparable Si content.

In experiments with the (MgO+G) isolation sleeves, the composition of pyrrhotite was found to change with temperature from the initial stoichiometric FeS to $Fe_{0.89}S$ at 1250 °C and $Fe_{0.85}S$ at 1450 °C (Table 3). At higher temperatures, sulfide melted and crystallized as pyrite and pyrrhotite during the quench (Table 3). Microscopic and X-ray analyses of the run products showed that pyrite content in the quenched aggregate increased with temperature from 20 vol.% at 1600 °C to 45 vol.% at 1800 °C. Based upon these data it was established that with an increase in temperature, the content of sulfur in sulfide melt increased. Moreover, a regular increase of sulfur content in sulfides, irrespective of their aggregate state was found for the entire range of temperatures from 1250 to 1800 °C (Fig. 9c). Remarkably, experiments, performed with the (MgO+BN) isolation sleeves, did not exhibit this tendency. In this case, only pyrrhotite formed from sulfide melt during quenching. Analysis of the quench pyrrhotite composition demonstrated that no

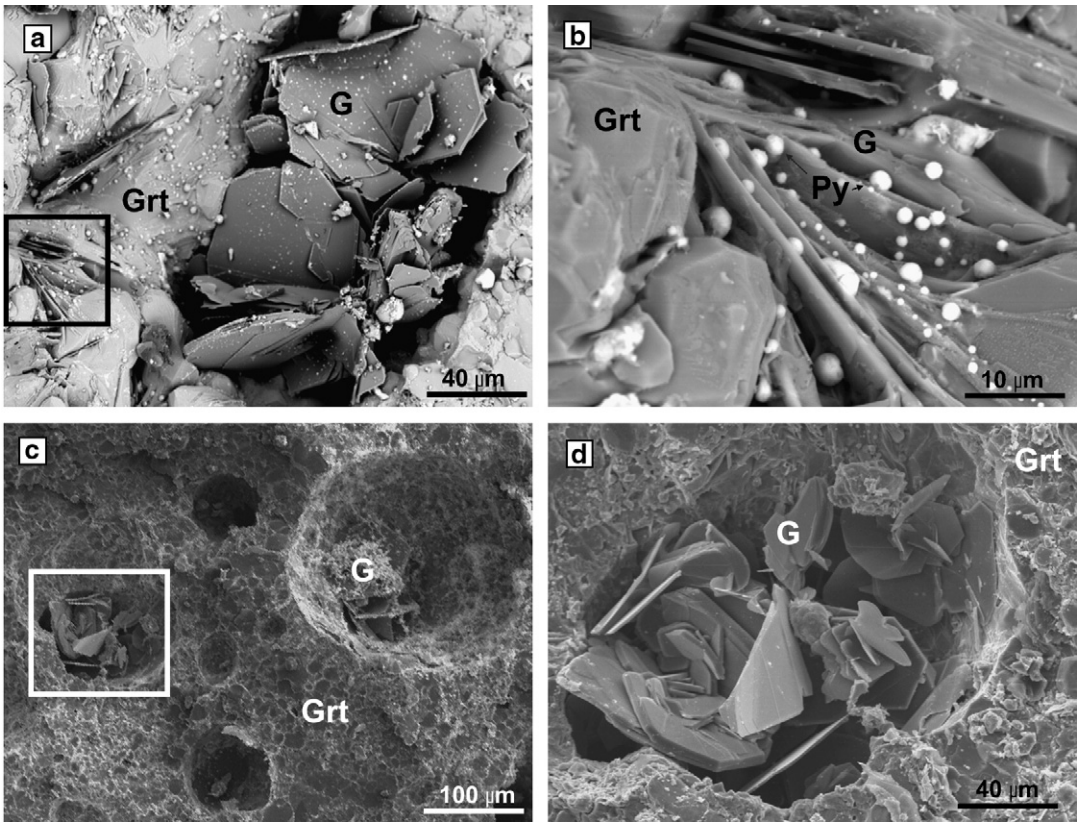

Fig. 8. SEM micrographs: a — cavities with graphite crystals and pyrite spheres (run 91/8, 1800 °C); b — intergrowth of garnet with graphite and pyrite spheres, an expanded fragment of the Fig. a; c — a fragment of carbonate–silicate ampoule with cavities (run 91/8, 1800 °C); d — graphite crystals in a cavity, expanded fragment of the Fig. c. Grt — garnet, Py — pyrite, G — graphite.

enrichment of sulfide melt with sulfur occurred in these experiments (Fig. 9c).

3.3. IR characterization of diamonds and carbon isotope analysis

For the infrared absorption measurements a number of spontaneously nucleated diamond crystals with appropriate sizes and quality were selected from runs 92/8 and 90/8 carried out at 1650 °C and 1700 °C, respectively. Typical IR spectra recorded for these diamonds are shown in Fig. 10. As it is seen from the spectra in the defect-induced one-phonon region (1400–900 cm^{-1}) the samples exhibit relatively strong absorption caused by nitrogen impurity. Absorption bands due to single substitutional nitrogen atoms, or C centers (a band peaking at 1130 cm^{-1}) and pairs of nearest-neighboring nitrogen atoms, or A centers (a band peaking at 1280 cm^{-1}) are present, so that the crystals correspond to mixed Ib–IaA type. Nitrogen concentrations were determined by decomposing the IR spectra, in the one-phonon region, into A and C components and using conversion factors of 16.5 atomic ppm cm^{-1} of absorption at 1280 cm^{-1} for the A centers (Boyd et al., 1994a,b) and 25 atomic ppm cm^{-1} of absorption at 1130 cm^{-1} for the C centers (Kiflawi et al., 1994). For the spectra presented in Fig. 10 calculations give nitrogen concentrations of 350–450 ppm and 1150–1050 ppm in the form of A and C centers, respectively. The total nitrogen content is approximately 1500 ppm. It is remarkable that, as in case of diamonds grown using a variety of non-metallic systems (Kanda et al., 1999; Borzdov et al., 2002; Pal'yanov et al., 2002b, 2004), diamond crystals synthesized in this study contain relatively high nitrogen concentrations at the level of typical values found in natural type Ia diamonds.

Another absorption feature present in the measured IR spectra is a sharp peak at 3107 cm^{-1}. As is known this absorption peak is related to hydrogen impurity in the diamond lattice and attributed to a C–H bond stretching vibration (Woods and Collins, 1983; De

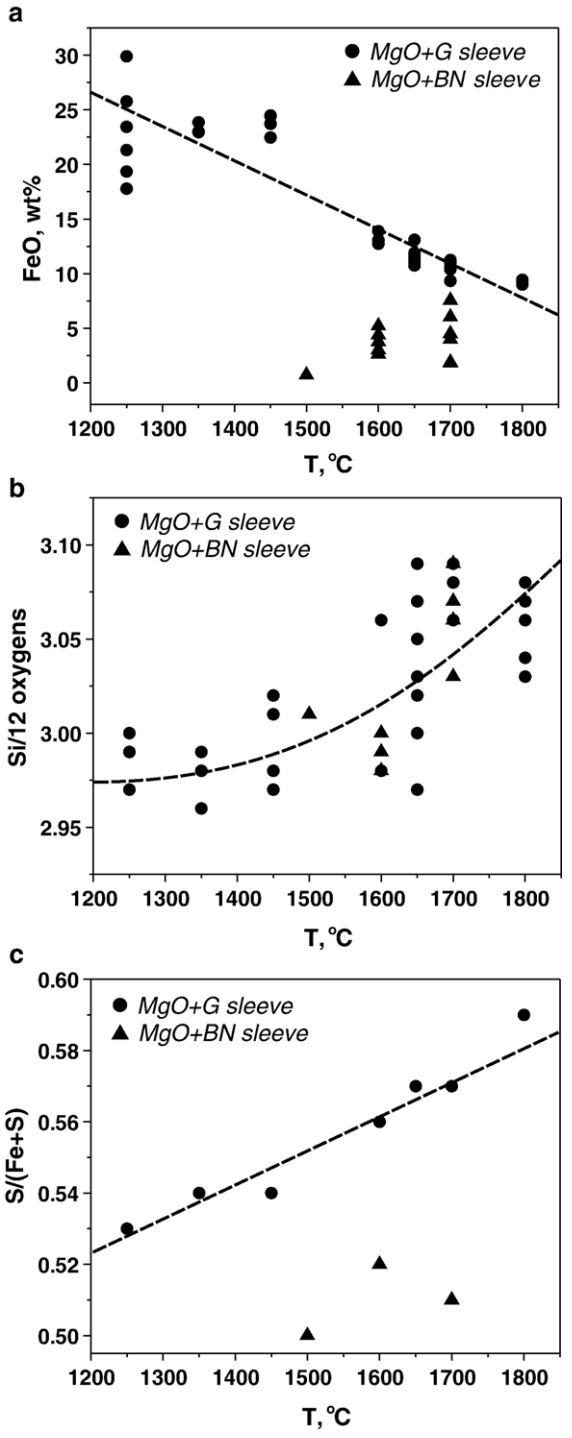

Fig. 9. Temperature dependence of the phases composition (6.3 GPa, 1250–1800 °C): a — FeO content in garnets; b — Si content per 12 oxygens in garnets; c — S content in sulfides: pyrrhotite (1250–1450 °C) and quenched pyrite–pyrrhotite aggregate (1600–1800 °C).

Werdt et al., 2003). The occurrence of hydrogen-related absorption features in the examined crystals indicates that hydrogen was present in the growth environment and was able to incorporate in diamonds during the growth.

For the reconstruction of diamond and graphite formation processes, analysis of carbon isotopic composition of the initial and final carbon-containing phases is of interest. Carbon isotope compositions of the initial magnesite ($\delta^{13}C=-0.1‰$) and graphite used for isolation sleeves ($\delta^{13}C=-27‰$) differed considerably. Isotopic analysis of final carbon-containing phases was performed with the experiment carried out at 1700 °C (run 90/8). It was established that spontaneously nucleated diamond had $\delta^{13}C=-7.3‰$, and $\delta^{13}C$ values of newly formed graphite varied from −0.06‰ to −3.7‰. Isotopic composition of graphite of the isolation sleeve after experiment changed slightly with $\delta^{13}C$ ranging from −25.3 to −26.8‰. This indicates that during the experiment some isotopic interchange between CO_2-fluid and carbon of the graphite sleeve took place. Consequently, considering the source of carbon for crystallized diamond both magnesite and graphite of the isolation sleeve should be taken into account. Besides, another potential source of carbon could be seed diamond crystals. However in experiments where spontaneous nucleation of diamond was established, the seed crystals did not undergo dissolution but exhibited diamond overgrowths. Therefore, at least for spontaneously nucleated diamonds, diamond

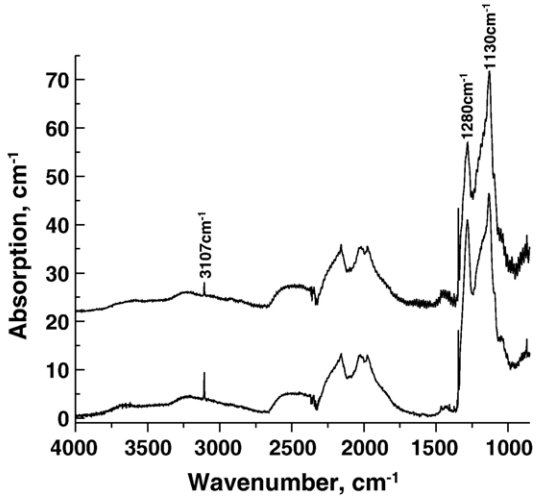

Fig. 10. Typical infrared absorption spectra of diamond crystals synthesized in the $MgCO_3$–SiO_2–Al_2O_3–FeS system at 1650–1700 °C. The spectra have been displaced for clarity.

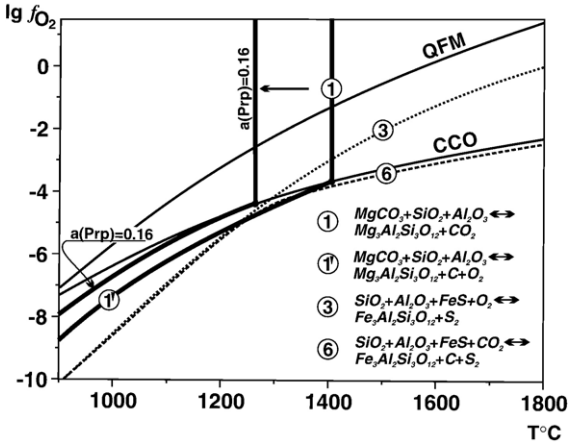

Fig. 11. Calculated logf_{O_2}–T diagram for the $MgCO_3$–SiO_2–Al_2O_3–FeS–C system at 6.3 GPa. 1, 1′, 3, 6 — invariant reactions; QFM, CCO — buffer equilibria; a(Prp) — activity of pyrope.

seed crystals can be ruled out as the possible source of carbon. An estimation of the carbon contribution from magnesite and graphite of the sleeve to the crystallized diamonds can be made with an assumption that no isotope fractionation occurred between the carbon-containing phases and neglecting the change of the isotope composition of graphite. It yields that isotope composition with $\delta^{13}C=-7.3‰$ could form due to mixing 27 wt.% of carbon from graphite used for isolation sleeves and 73 wt.% of carbon from carbonate. This estimation shows that diamond, as well as metastable graphite, crystallized in the experiments, were formed mainly from carbon of the initial magnesite.

4. Processes of carbonate–oxide–sulfide interaction and diamond-forming mechanism

Thermodynamic calculations were performed with the $MgCO_3$–Al_2O_3–SiO_2–FeS–C–O_2–H_2 system at 6.3 GPa and temperatures in the range 900–1800 °C. Since the equilibrium was not attained in most of the experiments (especially in those at low temperatures) the calculations were mainly intended for the analysis of general regularities of the carbonate–oxide–sulfide interaction, and were not aimed at interpreting all the peculiarities of the formation and composition of phases produced in experiments. A "Selektor-C" computer program (version 3.11, 1997) (Chudnenko et al., 1995; Karpov et al., 2002), employing Gibbs free energy minimization, was used for the calculations. This software is calibrated for the upper mantle conditions. Initial thermodynamic data for the solid phases, FeS melt and gases were taken from g_reid, c_hol, c_sprons databases, available in the "Selektor-C" program, and corrected as shown in (Konnikov and Palyanova, 2000; Sokol et al., 2000). For the solid phases a model of ideal type of activity of the endmembers was employed. The C–O–H–S fluid was approximated by an ideal mixture of real gases (H_2, CH_4, H_2O, CO_2, CO, COS, CS_2, SO_2, S_2, O_2). Model composition of the system was set in accord with the experiments or stoichiometry of the reactions involving $MgCO_3$, Al_2O_3, SiO_2, FeS, CO_2. In addition, we took into account possible presence of atmospheric oxygen, which can be adsorbed on the starting reagents and materials, and a possibility of hydrogen diffusion in the reaction ampoules during the experiments. Based on the data of (Pal'yanov et al., 2005b), the quantity of hydrogen in the system was estimated to be not higher than 0.1 wt.%. The results of the calculations, constituting the invariant reactions and composition of fluid in equilibrium with diamond are presented in Fig. 11 and Table 4, respectively.

Based upon the experimental results and thermodynamic calculations we shall consider the major regularities of the processes, reactions and mechanisms responsible for the formation of carbon polymorphs (diamond and graphite) in association with Mg,Fe-silicates and sulfides, as observed in this study. We suppose that the elemental carbon could form in the experiments as a result of two processes, first, decarbonation of magnesite producing CO_2 and, second, carbon reduction due to reaction of CO_2 with pyrrhotite. Decarbonation of magnesite proceeds via the following main reaction:

$$3MgCO_3 + Al_2O_3 + 3SiO_2 \leftrightarrow Mg_3Al_2Si_3O_{12} + 3CO_2 \quad (1)$$

This reaction was studied experimentally by Knoche et al. (1999). As it follows from the determined location of the reaction boundary, at the pressure of 6.3 GPa magnesite decarbonation via reaction (1) proceeds at temperatures higher than 1400 °C. However our results suggest that decarbonation occurred in the experiments at temperatures as low as 1250 °C. This discrepancy urges us to consider possible factors which could shift reaction (1) to lower temperatures. It has been shown previously that an essential effect on the decarbonation is exerted by the presence of H_2O in the system (Ogasawara et al., 1997; Knoche et al., 1999). However, the starting reagents used in this study were dried up prior to experiments and did not contain considerable quantity of H_2O. Furthermore, should magnesite decarbonation be affected by adsorbed atmospheric H_2O, it might be expected that in

our low-temperature experiments, reaction (1) should have occurred throughout the carbonate–oxide ampoule. This, however, was not observed, and the effect of H_2O can be ruled out. Another important factor resulting in the temperature downshift is the reduction of activity of pyrope due to its dilution. In particular, thermodynamic calculation performed for pyrope–almandine–grossular garnet (similar in composition to the garnet from group I eclogites), with a(Prp)=0.16, yielded a decrease in the magnesite decarbonation temperature to approximately 1270 °C at 6.3 GPa (Knoche et al., 1999). We found that garnets from the experiments at 1250–1450 °C are characterized by high FeO content, up to 29.9 wt.% (Fig. 9, Table 2). For such concentrations of Fe in the Fe, Mg-garnet and with the excess mixing energy, W^{Grt}_{Fe-Mg} of 0.8 kJ mol^{-1} (Holland, Powell, 1998), the activity of pyrope, as follows from our calculations, decreases to a (Prp)=0.009. This implies that, in the presence of Fe-containing garnets, decarbonation reaction (1) could occur even at the temperature as low as 1250 °C. Transfer of iron from pyrrhotite to garnet proceeded via the reactions of pyrrhotite oxidation. As a result, sulfide was depleted with iron and enriched with sulfur. Almandine garnet formed by the scheme:

$$0.33x \cdot Al_2O_3 + x \cdot SiO_2 + FeS + 0.5x \cdot O_2 \rightarrow 0.33x \cdot Fe_3Al_2Si_3O_{12} + Fe_{1-x}S, \quad (2)$$

where $x>0$. For the calculations we used a simplified reaction in the form:

$$3SiO_2 + Al_2O_3 + 3FeS + 1.5O_2 \leftrightarrow Fe_3Al_2Si_3O_{12} + 1.5S_2 \quad (3)$$

In the low-temperature experiments, at 1250–1400 °C, where sulfide did not melt, conditions for the magnesite decarbonation via reaction (1) were realized only within the reaction zones, enriched with Fe^{2+} (Fig. 3). In experiments, carried out at higher temperatures, 1600–1800 °C, decarbonation occurred throughout the carbonate–oxide ampoule. Based on the experimental results, we suggest that in addition to the main reaction (1), following decarbonation reactions also took place:

$$MgCO_3 + SiO_2 \leftrightarrow MgSiO_3 + CO_2 \quad (4)$$

$$MgCO_3 + MgSiO_3 \leftrightarrow Mg_2SiO_4 + CO_2 \quad \text{(Newton and Sharp, 1975; Wyllie et al., 1983)} \quad (5)$$

Let us now consider the reduction of CO_2 with the formation of elemental carbon. Thermodynamic calculations show that diamond and graphite can form via CO_2 reduction by sulfide (Fig. 11):

$$3SiO_2 + Al_2O_3 + 3FeS + 1.5CO_2 = Fe_3Al_2Si_3O_{12} + 1.5C + 1.5S_2 \quad (6)$$

Taking into consideration the pyrrhotite composition from run at 1250 °C, this reaction can take the form of:

$$FeS + 0.0367Al_2O_3 + 0.11SiO_2 + 0.055CO_2 \rightarrow Fe_{0.89}S + 0.0367Fe_3Al_2Si_3O_{12} + 0.055C \quad (7)$$

In experiments at 1250–1400 °C, the formation of carbon by the reaction (6) was localized within the reaction zone. At higher temperatures, 1600–1800 °C, the process of the elemental carbon formation took place throughout the entire reaction volume. It is necessary to note that in this temperature range CO_2 was reduced to elemental carbon by sulfide melt. Reaction (6) took place at fO_2 close to CCO buffer (Fig. 11). As a result, sulfide melt was enriched with sulfur, and crystallized as pyrite–pyrrhotite aggregates during quenching.

The decarbonation reactions, releasing CO_2, transport of Fe from sulfide to the carbonate–oxide substrate and CO_2 reduction took place almost in parallel. This caused the formation of intergrowth aggregates of graphite and garnet (Fig. 8b) and graphite inclusions in garnet crystals. Fluid, composed mainly of CO_2, was the media, which could provide transport of the components. The occurrence in the cavities of euhedral crystals of garnet, coesite, graphite and diamond, as well as pyrite spheres, are evidence for their crystallization from fluid, and, consequently, for significant solubility of these phases in CO_2-fluid at the experimental conditions.

It is worth of considering if other processes could lead to crystallization of graphite and diamond in our experiments. It was found previously that in prolonged experiments with CO_2-fluid at high P–T parameters, crystallization of graphite due to CO_2 reduction frequently occurred (Jakobsson and Oskarsson, 1994; Brooker et al., 1998). This process is caused by the diffusion of hydrogen through the capsule walls. Intensity and direction of hydrogen diffusion depend on the fluid composition, material of the capsule, hydrogen fugacity in the cell materials and run duration. In this connection, for the experimental investigation of carbonate–silicate reactions, a double capsule buffering method is often applied. The purpose of this method is

to preserve low hydrogen fugacity in the sample and thus to prevent the reduction of carbonates and CO_2 by hydrogen (Brey et al., 1983). However, it is impossible to apply this method for studying sulfide-containing systems at relatively high temperatures. Previously we have studied the decarbonation reaction in the $MgCO_3$–SiO_2–Al_2O_3 system at 6.0 GPa and 1600 °C without buffering (Pal'yanov et al., 2005b). When Pt-capsules were opened after 40 h experiments it was established that gaseous phase, consisted mainly of CO_2, contained from 6.4 to 11.8 mol% H_2O. Concentration of gaseous phase in the system was up to 2.4–3.4 wt.%. Therefore, it is possible that in experiments performed in the present study, hydrogen could spontaneously diffuse to the sample. A direct indication of hydrogen presence in the reaction volume is the observation of hydrogen-related absorption features in the IR spectra of the crystallized diamonds. However, the amount of carbon released due to CO_2 reduction by diffused-in hydrogen was too small to produce a significant supersaturation of the system, required for diamond nucleation (Pal'yanov et al., 2005b). Our calculations show that at T = 1250 °C the concentration of H_2O (the product of reaction of H_2 with CO_2) in the fluid phase of the $MgCO_3$–Al_2O_3–SiO_2–FeS–C system (containing 0.1 wt.% H_2) is 25 wt.%, and at $T \geq 1350$ °C it decreases to 6 wt.% (Table 4).

The composition of silicates, formed in the studied system, depends on the specific features of the processes considered above. The established trends of Fe-content in garnets are determined, first of all, by the change of sulfur concentration in sulfide (sulfide melt), redox potential in the system and by the degree of magnesite decarbonation. Earlier, in experiments at 5.0 GPa and 1800–2200 °C, it was shown that with an increase in the content of sulfur in sulfide melt to a value higher than that of FeS stoichiometry, the partition coefficient of Fe between sulfide and silicates ($D^{sulf/sil}$) increased (Jana and Walker, 1997). In the present experiments, small volume of the reaction zone and slight oxidation of pyrrhotite at 1250–1450 °C did not lead to a significant increase in sulfur concentration in sulfide (Fig. 9c), resulting in low $D^{sulf/sil}$ and, hence, high Fe-content in garnets (Fig. 9a). At temperatures of 1600–1800 °C, due to high degree of $MgCO_3$ decarbonation and considerable increase in sulfur concentration in sulfide melt, Fe-content in silicates decreased to 9–13 wt.%.

In experiments with the (MgO + BN) isolation sleeves, oxygen fugacity in the samples was close to IW buffer (Wendlandt and Huebner, 1982). Low oxygen fugacity in the system resulted in low Fe-content in silicates (Fig. 9a). Oxidation of pyrrhotite did not take place and sulfur concentration in sulfide did not increase (Fig. 9c). CO_2 formed through magnesite decarbonation was reduced to carbon by interaction with boron nitride. BN oxidation products ($Mg_3B_2O_6$ and $Mg_2B_2O_5$) were found by X-ray analysis.

Finally, it is reasonable to suppose that the most probable mechanism of diamond (or graphite) crystallization in the experiments with the (MgO + G) isolation sleeves was as follows. CO_2-fluid produced through the decarbonation reactions, dissolved the initial oxides, sulfide, carbonate and newly formed silicates. Reduced carbon was also dissolved in CO_2 and after supersaturated carbon solution was formed in the fluid, it became possible for diamond or metastable graphite to crystallize in the cavities or intergranular space of the silicate or silicate–sulfide matrix. Saturation of the fluid with carbon to a level necessary for diamond or graphite crystallization to start was achieved through the oxidation–reduction reactions between sulfide and CO_2. Surplus quantity of sulfide in experiments provided gradual and continual saturation of the system with carbon.

5. Summary and conclusions

The results of experiments performed in the present study are evidence for a particular role of sulfides — as an agent able to reduce CO_2 to elemental carbon: diamond or graphite. It is important that sulfides act as reducing agents both in melted and solid states. As a result of the carbonate–oxide–sulfide interaction in the $MgCO_3$–SiO_2–Al_2O_3–FeS system, diamond or graphite form in association with garnet, orthopyroxene, coesite and sulfides (pyrrhotite and pyrite). The source of carbon for diamond and graphite is $MgCO_3$. Taking into account the abundance of sulfides in diamondiferous mantle xenoliths, and in inclusions in diamonds from kimberlites, the model of diamond formation, which accounts for the reducing role of sulfides, may be of relevance to the diamond genesis in the mantle. Findings of sulfides in micro-inclusions in metamorphic diamonds (Hwang et al., 2001, 2003) suggest that this model may also hold for UHP metamorphic processes.

It is found that the composition of sulfides changes in the course of carbonate–oxide–sulfide interaction. Pyrrhotite is enriched with S and depleted with Fe, and, in case of sulfide melt, pyrite and pyrrhotite form during quenching. Therefore, findings of sulfides with relatively high S/(S + Me) ratios (Klein-BenDavid et al., 2003) or pyrite in diamondiferous xenoliths (Ragozin et al., 2006) or in inclusions in diamond (Bulanova et al., 1982; Deines and Harris, 1995) may be taken as indicators of the processes investigated in this study.

The carbonate–oxide–sulfide interaction, studied in this work, can be considered as one of the possible scenarios of the mantle metasomatism. CO_2-fluid, formed via the decarbonation reactions, acts as a metasomatic agent, providing transport of dissolved components, including silicates, carbonates, sulfides and carbon. The role of CO_2 as one of the prevailing components of the deep fluids has been discussed in a number of studies (Andersen and Neumann, 2001; Scambelluri and Philippot, 2001). Findings of CO_2 inclusions in diamond (Schrauder and Navon, 1993) are direct evidence for the existence of CO_2 in the mantle.

Finally, summarizing the results of the present study, the following conclusions can be made:

1. Interaction in the $MgCO_3$–SiO_2–Al_2O_3–FeS system proceeds via reactions of decarbonation and reduction of CO_2 to elemental carbon, finally, resulting in the formation of an association of Mg,Fe-silicates, sulfides and graphite or diamond. The source of carbon for diamond and graphite is the initial carbonate.
2. In the course of carbonate–oxide–sulfide interaction sulfides act as reducing agents irrespective of their aggregate state. Due to formation of Mg,Fe-silicates, considerable enrichment of pyrrhotite with sulfur and depletion with iron take place. At temperatures higher than pyrrhotite liquidus, sulfide melt crystallizes during quenching as pyrite and pyrrhotite, and at temperatures lower than the liquidus, pyrrhotite stoichiometry changes from FeS to $Fe_{0.85}S$.
3. Diamond or graphite crystallize from CO_2-dominated fluid, supersaturated with carbon and contained dissolved silicates, oxides and sulfides. The driven force of the elemental carbon crystallization is the oxidation–reduction reactions occurring under carbonate–oxide–sulfide interaction.
4. The stable growth form of diamond produced in the experiments is octahedron. Diamond crystals are found to contain nitrogen impurity in single substitutional (C-centers) and paired (A-centers) forms with concentrations of 1050–1150 ppm and 350–450 ppm, respectively, as well as hydrogen-related centers.
5. The investigated processes and mechanisms of diamond formation in the course of carbonate–oxide–sulfide interaction can be one of the possible models of the diamond genesis in the processes of mantle metasomatism or UHP metamorphism of crustal material.

Acknowledgements

The authors are grateful to A.F. Khokhryakov and A.G. Talibova for their assistance in the course of the work. Two anonymous reviewers are thanked for their in-depth reviews that considerably improved this manuscript. The support from the Russian Foundation for Basic Research (grant No. 06-05-64576) is acknowledged.

Appendix A. Supplementary data

Supplementary data associated with this article can be found, in the online version, at doi:10.1016/j.epsl.2007.05.033.

References

Akaishi, M., Kanda, H., Yamaoka, S., 1990. Synthesis of diamond from graphite–carbonate systems under very high temperature and pressure. J. Cryst. Growth 104, 578–581.

Akaishi, M., Kumar, M.S.D., Kanda, H., Yamaoka, S., 2000. Formation process of diamond from supercritical H_2O–CO_2 fluid under high pressure and high temperature conditions. Diamond Relat. Mater. 9, 1945–1950.

Andersen, T., Neumann, E.-R., 2001. Fluid inclusions in mantle xenolines. Lithos 55, 301–320.

Arima, M., Nakayama, K., Akaishi, M., Yamaoka, S., Kanda, H., 1993. Crystallization of diamond from a silicate melt of kimberlite composition in high-pressure and high-temperature experiment. Geology 219, 68–970.

Arima, M., Kozai, Y., Akaishi, M., 2002. Diamond nucleation and growth by reduction of carbonate melts under high-pressure and high-temperature conditions. Geology 30, 691–694.

Borzdov, Yu.M., Pal'yanov, Yu.N., Kupriyanov, I.N., Gusev, V.A., Khokhryakov, A.F., Sokol, A.G., Efremov, A.V., 2002. HPHT synthesis of diamond with high nitrogen content from a Fe_3N–C system. Diamond Relat. Mater. 11, 1863–1870.

Boyd, S.R., Kiflawi, I., Woods, G.S., 1994a. The relationship between infrared absorption and the A defect concentration in diamond. Philos. Mag., B 69, 1149–1153.

Boyd, S.R., Pineau, F., Javoy, M., 1994b. Modeling the growth of natural diamonds. Chem. Geol. 116, 29–42.

Brey, G., Brice, W.R., Ellis, D.J., Green, D.H., Harris, K.L., Ryabchikov, I.D., 1983. Pyroxene–carbonate reactions in the upper mantle. Earth Planet. Sci. Lett. 62, 63–74.

Brooker, R., Holloway, J.R., Hervig, R., 1998. Reduction in piston-cylinder experiments: the detection of carbon infiltration into platinum capsules. Am. Mineral. 83, 985–994.

Bulanova, G.P., 1995. Formation of diamond. J. Geochem. Explor. 53, 1–23.

Bulanova, G.P., Shestakova, O.E., Leskova, N.V., 1982. Sulfide inclusions in Yakitian diamonds. Zap. Vses. Mineral. Obsestva 111 (5), 300–310 (in Russian).

Bulanova, G.P., Barashkov, Yu.P., Talnikova, S.B., Smirnova, G.D., 1993. Natural Diamond-Genetic Aspects. Nauka, Novosibirsk. (in Russian).

Chudnenko, K.V., Karpov, I.K., Bychinski, V.A., Kulik, D.A., 1995. Current status of the SELEKTOR soft package. In: Kharaka, Y.K., Chudaev, O.V. (Eds.), Proceedings of the 8th International Symp. on Water–Rock Interaction, Vladivostok, Russia. Balkema, Rotterdam, pp. 725–727.

De Werdt, F., Pal'yanov, Yu.N., Collins, A.T., 2003. Absorption spectra of hydrogen in ^{13}C diamond produced by high-pressure, high-temperature synthesis. J. Phys., Condens. Matter 15, 3163–3170.

Deines, P., Harris, J.W., 1995. Sulfide inclusion chemistry and carbon isotopes of African diamonds. Geochim. Cosmochim. Acta 59, 3173–3188.

Dobrzhinetskaya, L.F., Green, H.W., Bozhilov, K.N., Mitchell, T.E., Dickerson, R.M., 2003. Crystallization environment of Kazakhstan microdiamond: evidence from nanometric inclusions and mineral associations. J. Metamorph. Geol. 21, 425–437.

Efimova, E.S., Sobolev, N.V., Pospelova, L.N., 1983. Sulphide inclusions in diamonds and features of their parageneses. Zap. Vses. Mineral. Obsestva 112 (3), 300–310. (in Russian).

Gasparik, T., 2002. Experimental investigation of the origin of majoritic garnet inclusions in diamonds. Phys. Chem. Miner. 29, 170–180.

Gunn, S.C., Luth, R.W., 2006. Carbonate reduction by Fe–S–O melts at high pressure and high temperature. Am. Mineral. 91, 1110–1116.

Haggerty, S.E., 1986. Diamond genesis in a multiply-constrained model. Nature 320, 34–38.

Harris, J.W., 1992. Diamond geology. In: Field, J.E. (Ed.), Properties of natural and synthetic diamond. Academic Press, London, pp. 345–389.

Harris, J.W., Gurney, J.J., 1979. Inclusions in diamond. In: Field, J.E. (Ed.), Properties of diamond. Academic Press, London, pp. 556–591.

Hwang, S.-L., Shen, P., Chu, H.-T., Yui, T.-F., 2001. Genesis of microdiamonds from melt and associated multiphase inclusions in garnet of ultrahigh-pressure gneiss from Erzgebirge, Germany. Earth Planet. Sci. Lett. 188, 9–15.

Hwang, S.-L., Shen, P., Yui, T.-F., Chu, H.T., 2003. Metal–sulfur–COH–silicate fluid mediated diamond nucleation in Kokchetav ultrahigh-pressure gneiss. Eur. J. Mineral. 15, 503–511.

Hwang, S.-L., Shen, P., Chu, H.-T., Yui, T.-F., Liou, J.G., Sobolev, N.V., Shatsky, V.S., 2005. Crust-derived potassic fluid in metamorphic microdiamond. Earth Planet. Sci. Lett. 231, 295–306.

Izraeli, E.S., Harris, J.W., Navon, O., 2001. Brine inclusions in diamonds: a new upper mantle fluid. Earth Planet. Sci. Lett. 187, 1–10.

Jakobsson, S., Oskarsson, N., 1994. The system C–O in equilibrium with graphite at high pressure and temperature: an experimental study. Geochim. Cosmochim. Acta 58, 9–17.

Jana, D., Walker, D., 1997. The influence of sulfur on partitioning of siderophile elements. Geochim. Cosmochim. Acta 61, 5255–5277.

Kanda, H., Akaishi, M., Yamaoka, S., 1999. Synthesis of diamond with the highest nitrogen concentration. Diamond Relat. Mater. 8, 1441–1443.

Karpov, I.K., Chudenko, K.V., Kulik, D.A., Bychinskii, V.A., 2002. The convex programming minimization of five thermodynamic potentials other that Gibbs energy in geochemical modeling. Am. J. Sci. 302, 281–311.

Kiflawi, I., Mayer, A.E., Spear, P.M., Van Wyk, J.A., Woods, G.S., 1994. Infrared absorption by single nitrogen and A defect centres in diamond. Philos. Mag., B 69, 1141–1147.

Klein-BenDavid, O., Logvinova, A.M., Izraeli, E., Sobolev, N.V., Navon, O., 2003. Sulfide melt inclusions in Yubileinaya (Yakutia) diamonds. 8th Int. Kimber. Conf., Exten. Abstr. FLA_0111, Victoria, Canada.

Klein-BenDavid, O., Wirth, R., Navon, O., 2006. TEM imaging and analysis of microinclusions in diamonds: a close look at diamond-growing fluids. Am. Mineral. 91, 353–365.

Knoche, R., Sweeney, R.J., Luth, R.W., 1999. Carbonation and decarbonation of eclogites: the role of garnet. Contrib. Miner. Petrol. 135, 332–339.

Konnikov, E.G., Palyanova, G.A., 2000. The effect of aqueous-carbon dioxide fluid on the pyrrhotite melting point. Geokhimiya, JAN 92–101.

Litvin, Yu.A., Zharikov, V.A., 2000. Experimental modeling of diamond genesis: diamond crystallization in multicomponent carbonate-silicate melts at 5–7 GPa and 1200–1570 °C. Dokl. Earth Sci. 373, 867–870.

Litvin, Yu.A., Chudinovskikh, L.T., Zharikov, V.A., 1997. Experimental crystallization of diamond and graphite from alkali–carbonate melts at 7–11 GPa. Dokl. Earth Sci. 355À, 908–912.

Litvin, Yu.A., Butvina, V.G., Bobrov, A.V., Zharikov, V.A., 2002. The first synthesis of diamond in sulfide–carbon systems: the role of sulfides in diamond genesis. Dokl. Earth Sci. 382, 40–44.

Luth, R.W., 1999. Carbon and carbonates in mantle. In: Fei, Y., Bertka, M.C., Mysen, B.O. (Eds.), Mantle Petrology: Field observation and high pressure experimentation: A tribute to Francis R. (Joe) Boyd. The Geochemical Society, Special Publication, vol. 6, pp. 297–316.

Marx, P.C., 1972. Pyrrhotine and the origin of terrestrial diamonds. Mineral. Mag. 38, 636–638.

Meyer, H.O.A., 1987. Inclusions in diamond. In: Nixon, H.P. (Ed.), Mantle xenoliths. John Wiley and Sons, New York, pp. 501–523.

Navon, O., Hutcheon, I.D., Rossman, G.R., Wasserburg, G.J., 1988. Mantle-derived fluids in diamond micro-inclusions. Nature 335, 784–789.

Newton, R.C., Sharp, W.E., 1975. Stability of forsterite + CO_2 and its bearing on the role of CO_2 in the mantle. Earth Planet. Sci. Lett. 26, 239–244.

Ogasawara, Y., Liou, J.G., Zhang, R.Y., 1997. Thermochemical calculation of log fO_2-TP stability relations of diamond-bearing assemblages in the model system CaO–MgO–SiO_2–H_2O. Geol. Geofiz. 38, 546–557.

Pal'yanov, Yu.N., Khokhryakov, A.F., Borzdov, Yu.M., Sokol, A.G., Gusev, V.A., Rylov, G.M., Sobolev, N.V., 1997. Growth conditions and real structure of synthetic diamond crystals. Geol. Geofiz. 38, 882–906.

Pal'yanov, Yu.N., Sokol, A.G., Borzdov, Yu.M., Khokhryakov, A.F., Sobolev, N.V., 1998. Diamond crystallization in the systems $CaCO_3$–C, $MgCO_3$–C, and $CaMg(CO_3)_2$–C. Dokl. Akad. Nauk 363, 230–233.

Pal'yanov, Yu.N., Sokol, A.G., Borzdov, Yu.M., Khokhryakov, A.F., Sobolev, N.V., 1999. Diamond formation from mantle carbonate fluids. Nature 400, 417–418.

Pal'yanov, Yu.N., Borzdov, Yu.M., Kupriyanov, I.N., Gusev, V.A., Khokhryakov, A.F., Sokol, A.G., 2001. High pressure synthesis and characterization of diamond from sulfur–carbon system. Diamond Relat. Mater. 10, 2145–2152.

Pal'yanov, Yu.N., Sokol, A.G., Borzdov, Yu.M., Khokhryakov, A.F., 2002a. Fluid-bearing alkaline–carbonate melts as the medium for the formation of diamonds in the Earth's mantle: an experimental study. Lithos 60, 145–159.

Pal'yanov, Yu.N., Sokol, A.G., Borzdov, Yu.M., Khokhryakov, A.F., Sobolev, N.V., 2002b. Diamond formation through carbonate–silicate interaction. Am. Mineral. 87, 1009–1013.

Pal'yanov, Yu.N., Borzdov, Yu.M., Sokol, A.G., Khokhryakov, A.F., Kupriyanov, I.N., 2004. Experimental studies of diamond formation processes in the modeling systems. The 55th Diamond Conf. Warwick. Abstract no. 20.1.

Pal'yanov, Yu.N., Sokol, A.G., Sobolev, N.V., 2005a. Experimental modeling of mantle diamond-forming processes. Russ. Geol. Geophys. 46, 1271–1284.

Pal'yanov, Yu.N., Sokol, A.G., Tomilenko, A.A., Sobolev, N.V., 2005b. Conditions of diamond formation through carbonate–silicate interaction. Eur. J. Mineral. 17, 207–214.

Palyanov, Yu.N., Borzdov, Yu.M., Khokhryakov, A.F., Kupriyanov, I.N., Sobolev, N.V., 2006. Sulfide melts–graphite interaction at HPHT

conditions: Implications for diamond genesis. Earth Planet. Sci. Lett. 250, 269–280.

Pearson, D.G., Shirey, S.B., Harris, J.W., Carlson, R.W., 1998. Sulphide inclusions in diamonds from the Koffiefontein kimberlite, S Africa: constraints on diamond ages and mantle Re–Os systematics. Earth Planet. Sci. Lett. 169, 311–326.

Ragozin, A.L., Shatsky, V.S., Zedgenizov, D.A., Mityukhin, S.I., 2006. Evidence for evolution of diamond crystallization medium in eclogite xenolith from the Udachnaya kimberlite pipe, Yakutia. Dokl. Earth Sci. 407A, 465–469.

Richardson, S.H., Shirey, S.B., Harris, J.W., 2004. Episodic diamond genesis at Jwaneng, Botswana, and implication for Kaapvaal craton evolution. Lithos 77, 143–154.

Sato, K., Katsura, T., 2001. Sulfur: a new solvent-catalyst for diamond synthesis under high-pressure and high-temperature conditions. J. Cryst. Growth 223, 189–194.

Sato, K., Akaishi, M., Yamaoka, S., 1999. Spontaneous nucleation of diamond in the system $MgCO_3$–$CaCO_3$–C at 7.7 GPa. Diamond Relat. Mater. 8, 1900–1905.

Scambelluri, M., Philippot, P., 2001. Deep fluids in subduction zones. Lithos 55, 213–227.

Schrauder, M., Navon, O., 1993. Solid carbon dioxide in a natural diamond. Nature 365, 42–44.

Schrauder, M., Navon, O., 1994. Hydrous and carbonatitic mantle fluids in fibrous diamonds from Jwaneng, Bostwana. Geochim. Cosmochim. Acta 58, 761–771.

Sharp, W.E., 1966. Pyrrhotite; a common inclusion in South African diamonds. Nature 211, 402–403.

Sharp, W.E., 1969. Melting curves of sphalerite, galena, and pyrrhotite and the decomposition curve of pyrite between 30 and 65 kilobars. J. Geophys. Res. 74 (6), 1645–1652.

Shatskii, A.F., Borzdov, Yu.M., Sokol, A.G., Pal'yanov, Yu.N., 2002. Phase formation and diamond crytsllization in carbon-bearing ultrapotassic carbonate–silicate systems. Geol. Geofiz. 43, 940–950.

Shatsky, V.S., Zedgenizov, D.A., Ragozin, A.L., Mityukhin, S.I., Sobolev, N.V., 2005. Evidence for metasomatic formation of diamond in eclogite xenolith from the Udachnaya kimberlite pipe (Yakutia). Dokl. Earth Sci. 402, 587–591.

Siebert, J., Guyot, F., Malavergne, V., 2005. Diamond formation in metal–carbonate interactions. Earth Planet. Sci. Lett. 229, 940–950.

Sobolev, N.V., 1977. The Deep-Seated Inclusions in Kimberlites and the Problem of the Composition of the Upper Mantle. American Geophysics Union, Washington.

Sobolev, N.V., Shatsky, V.S., 1990. Diamond inclusions in garnets from metamorphic rocks: a new environment for diamond formation. Nature 343, 742–746.

Sokol, A.G., Pal'yanov, Yu.N., Borzdov, Yu.M., Khokhryakov, A.F., Sobolev, N.V., 1999. Crystallization of diamond from silicate-fluid systems at P=7,0 GPa and T=1700–1750 °C. Dokl. Akad. Nauk 368, 954–957.

Sokol, A.G., Tomilenko, A.A., Pal'yanov, Y.N., Borzdov, Y.M., Pal'yanova, G.A., Khokhryakov, A.F., 2000. Fluid regime of diamond crystallisation in carbonate–carbon systems. Eur. J. Mineral. 12, 367–375.

Sokol, A.G., Pal'yanov, Yu.N., Pal'yanova, G.A., Khokhryakov, A.F., Borzdov, Yu.M., 2001. Diamond and graphite crystallization from COH fluids under high pressure and high temperature conditions. Diamond Relat. Mater. 10, 2131–2136.

Sokol, A.G., Pal'yanov, Yu.N., Pal'yanova, G.A., Tomilenko, A.A., 2004. Diamond crystallization in fluid and carbonate–fluid systems under mantle P–T conditions: 1. Fluid composition. Geochem. Int. 42, 830–838.

Spetsius, Z.V., 1999. Two generations of diamonds in eclogite xenoliths from Yakutia. In: Gurney, J.J., Gurney, J.L., Pascoe, M.D., Richardson, S.H. (Eds.), Proceedings of the 7th International Kimberlite Conference, Red Roof Design, Cape Town, pp. 823–828.

Taniguchi, T., Dobson, D., Jones, A.P., Rabe, R., Milledge, H.J., 1996. Synthesis of cubic diamonds in the graphite–magnesium carbonate and graphite–$K_2Mg(CO_3)_2$ systems at high pressure of 9–10 GPa region. J. Mater. Res. 11, 2622–2632.

Taylor, L.A., Anand, M., 2004. Diamonds: time capsules from the Siberian Mantle. Chem. Erde 64, 1–74.

Tomlinson, E.L., Jones, A.P., Harris, J.W., 2006. Co-existing fluid and silicate inclusions in mantle diamond. Earth Planet. Sci. Lett. 250, 581–595.

Wendlandt, R.F., Huebner, J.S., 1982. The redox potential of boron nitride and implications for its use as a crucible material in experimental petrology. Am. Mineral. 67, 170–174.

Woods, G.S., Collins, A.T., 1983. Infrared absorption spectra of hydrogen complexes in type Ia diamond. J. Phys. Chem. Solids 44, 471–475.

Wyllie, P.J., Huang, W.L., Otto, J., Byrnes, A.P., 1983. Carbonation of peridotites and decarbonation of siliceous dolomites represented in system CaO–MgO–SiO_2–CO_2 to 30 kbar. Tectonophysics 100, 359–388.

Yamaoka, S., Akaishi, M., Kanda, H., Osawa, T., 1992. Crystal growth of diamond in the system of carbon and water under very high pressure and temperature. J. Cryst. Growth 125, 375–377.

Yamaoka, S., Kumar, M.D.S., Kanda, H., Akaishi, M., 2002. Formation of diamond from $CaCO_3$ in a reduced C–O–H fluid at HP–HT. Diamond Relat. Mater. 11, 1496–1504.